analytical chemistry

pubs.acs.org/ac
Article

Chemical Analysis of Deep-Lung Fluid Derived from Exhaled Breath Particles

Tayeb Kakeshpour,* John M. Louis, Peter J. Walter, and Ad Bax*

Cite This: https://doi.org/10.1021/acs.analchem.4c06422
Read Online

ABSTRACT: Breath particles generated deep within the lung provide noninvasive access to sampling nonvolatiles in peripheral airway lining fluid. However, background contamination, their variable production among subjects, together with a huge unknown dilution when using the common breath condensate method for collection has limited their use for quantitative biomarker analysis. Instead, we first capture and dry the particles in a flexible chamber followed by accurate optical particle characterization during their collection for chemical analysis. By decoupling breathing and aerosol sampling airflows, this sequential approach not only accommodates all types of breathing routines but also enables the use of a variety of aerosol samplers for downstream biomarker analysis. Using ^{23}Na NMR, we measured 0.66 M Na in dry particles collected on a filter, which suggests that dehydration reduces their volume by a factor of ~ 5.5 based on known Na levels in lung fluid. ^{1}H NMR revealed 0.36 and 0.68 M phosphocholine lipids in dried particles collected from two volunteers, presumably enriched to these levels relative to literature values derived from bronchoalveolar lavage fluid due to the film-bursting mechanism that underlies breath particle generation. Decoupling of breath collection and aerosol capture enabled the design of an impactor sampler with 72% efficiency. This impactor minimizes reagent and handling-related contamination associated with traditional filters by collecting dry particles directly in a microreactor for subsequent derivatization and quantification by mass spectrometry. The method is demonstrated by quantifying subnanogram amounts of urea from breath particles, corresponding to lung fluid urea concentrations consistent with literature blood plasma values.

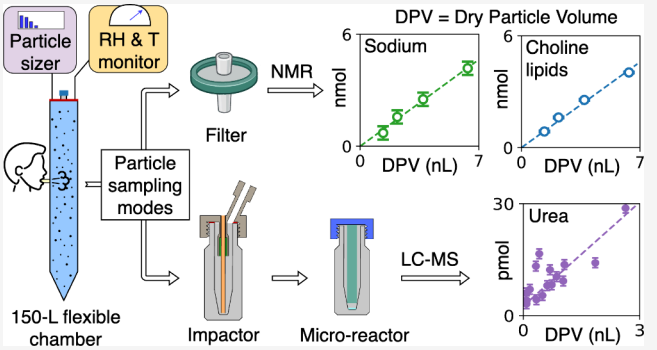

INTRODUCTION

Breath droplets generated during reopening of transiently closed small airways enable noninvasive sampling of the deep lung epithelial lining fluid (ELF).[1] Closure of small airways is associated with fluid surface tension when their diameter reduces during deep exhalation. Subsequent inhalation breaks open the occluded channels, which constitutes a potent mechanism of breath droplet generation.[2] As expected for this mechanism, deep exhalation results in greater narrowing of the airways and thereby increases the fraction of small airways that becomes transiently occluded. Consequently, this leads to an increase in reopenings during the next inhalation, drawing the breath particles into the alveoli prior to exhalation into the atmosphere. So, it is the depth of the preceding exhalation, rather than the final exhalation, that determines the number of exhaled particles. As shown by Johnson and Morawska, breath-holding prior to the final exhalation results in progressive loss of larger particles due to their sedimentation during such a breath hold.[2] Subsequently, Almstrand et al.[3,4] derived the closing volume in their subjects using N_2 measurements, proving that progressive closure of small airways increases breath particle production. These findings concur with the seminal work of Scheideler et al. (1993),[5] which demonstrated the presence of proteins in breath condensate that were absent in saliva samples of the same subjects from large sample collections. It is now widely accepted that breath droplets predominantly originate from the reopening of transiently closed small airways deep within the lung,[6] thus enabling noninvasive sampling of lung fluids.[7]

Although quantitative analysis of volatile components in breath condensate dates back to Linus Pauling's pioneering study in 1971,[8] the unknown dilution of nonvolatile components by water in exhaled breath condensate historically has limited their quantitative analysis.[9−11] This variable degree of dilution is dominated by large variations in droplet production between individuals, and even within the same individual at different times.[4,12,13] Further complicating this issue is the variable efficiency of typical condensation-based

Received: November 27, 2024
Revised: February 3, 2025
Accepted: February 6, 2025

https://doi.org/10.1021/acs.analchem.4c06422
Anal. Chem. XXXX, XXX, XXX−XXX

devices used to collect breath samples.[14] In 2009, Almstrand et al. introduced a method that characterizes breath particles using an optical particle sizer during their collection for subsequent chemical analysis,[15] allowing analyte measurements to be normalized to the volume of collected particles and thereby resolving the issue of unknown dilution. This approach is now increasingly adopted.[16]

Below the deliquescence relative humidity (DRH), respiratory aerosols are almost completely anhydrous. Above the DRH, they start to absorb water from the air and their size steeply rises with relative humidity (RH).[17,18] The DRH value for hygroscopic salts such as chloride salts of magnesium or calcium can be as low as 30%, but for typical salts it is in the range of 60−90%.[19] The DRH is about 75% for sodium chloride, which is the dominant salt in biological fluids. Indeed, for particles produced by deep exhalation maneuvers, Holmgren et al. measured the DRH to be 75%.[13] For reproducible particle sizing, airborne particles are best characterized below the deliquescence point, or the RH of the environment must be tightly regulated. The former approach is technically easier to achieve, particularly since RH depends strongly on temperature. For example, at 90% RH a 0.2 K uncertainty in temperature results in ∼1% uncertainty in RH. Moreover, optical particle sizing introduces heat into the system due to operating lasers and other electronics, which makes it difficult to establish the relevant temperature. However, studies also have been conducted under tightly controlled environmental conditions mimicking the human lung,[20] and measuring droplet size very close to the mouth.[21,22]

The very low fraction of airway lining fluid in exhaled breath condensate, typically in the 40−200 parts-per-million (ppm) range,[10] poses a challenge in reliable quantification of its composition. During tidal breathing, subjects typically produce only nanogram quantities of breath particles per liter of exhaled air.[23] Although breath particle production can be enhanced by more than an order of magnitude by the deep exhalation maneuver,[15,24] the collected samples remain exceptionally small, typically <1 μg total nonvolatile mass. Quantitative analysis of metabolites in such samples becomes especially challenging for molecules that are also present as contamination in solvents or reagents.[25] Therefore, contamination-free sample collection coupled with protocols that require minimal solvents and reagents are required for successful analysis of metabolites in exhaled breath particles. Furthermore, to obtain a reliable correlation between counted particles and measured analytes, the abundant background aerosols present in ambient air should be excluded during sample collection.

In this study, breath particles were first captured in a flexible chamber under controlled humidity conditions, ensuring measurements below their deliquescence point. The particles were then collected using either a home-built impactor device or a polytetrafluoroethylene (PTFE) filter, while monitoring their size using a commercial optical particle sizer. The total phosphatidylcholine lipids and sodium were quantified by NMR spectroscopy. Given that the tightly regulated sodium content in airway lining fluid is ∼122 mM,[26] quantitative measurement of the collected sodium allowed back-calculation of the aqueous volume from which the particles derived.

Additionally, an efficient particle impactor was developed for the collection of dry breath particles in a microreactor, enabling subsequent derivatization and quantification using liquid chromatography with in-line mass spectrometry (LC-MS). This method was applied to quantifying subnanogram amounts of urea, showing good agreement with values expected based on previously reported concentrations.

EXPERIMENTAL SECTION

Breath Sampling Setup. Samples generated by deep breathing maneuvers were collected in a static-shielding flexible chamber (Figure 1).[1] This chamber was adapted

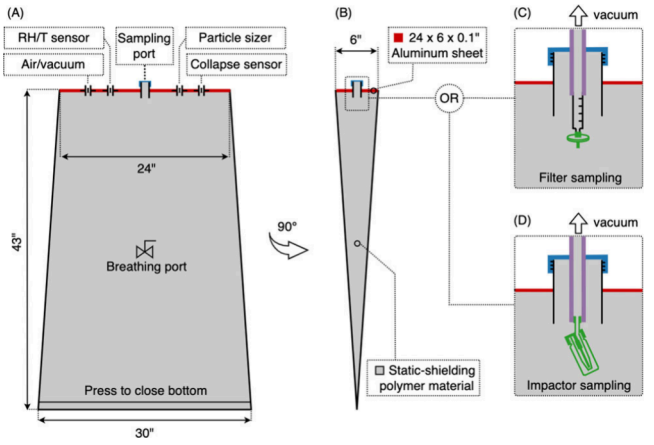

Figure 1. Aerosol collection chamber: (A) Front view; (B) Side view; (C) Filter collection configuration; and (D) Impactor collection configuration. See Experimental Section for details.

from a press-to-close polyethylene bag with an aluminized polyester middle layer (McMASTER-CARR, 4663T9), custom-made to the described dimensions. The chamber is equipped with five orifices supported by an aluminum sheet at the top, as shown in Figure 1: (1) an air/vacuum port for purging and prefilling the chamber with HEPA-filtered anhydrous air; (2) an RH and temperature (T) port for monitoring relative humidity with a capacitive sensor (HIH-5030, Honeywell) and temperature with a K-type thermocouple; (3) a 1-in. diameter sampling port designed to accommodate various aerosol sampling devices; (4) a particle sizer port connected to an optical particle sizer (TSI-3330) via conductive silicone tubing (TSI, 3001788); and (5) A collapse sensor port that signals a microcontroller by generating voltage when two copper pieces touch, which are mounted on opposite sides of the chamber, 5 in. from the top. The airflow for clean air and vacuum lines was adjusted using rotameter air flow controllers (UNION CARBIDE 24 and 50 L/min models), and their open/close status was electronically controlled by solenoid valves. A sampler rotameter was calibrated for operation under negative pressure conditions, generated by a diaphragm pump (PFEIFFER, MVP 040−2). A microcontroller facilitated programmable sampling, purging, and preparation of the chamber between measurements, controlled wirelessly by custom software running on an Android tablet.

The breathing port was positioned about 23 in. below the top of the chamber. This arrangement also served as a highly effective trap for saliva and any upper respiratory tract droplets larger than *ca.* 5 μm.[27] A manually operated rubber valve with an inner diameter of 0.5" was used for the breathing port. The entire system was set up in a clean air enclosure with total counts of ≥0.3 μm background particles being ≤5 L^{-1}.

Sample Production. Breath samples were collected under an exemption by the NIH Institutional Review Board (IRB

https://doi.org/10.1021/acs.analchem.4c06422
Anal. Chem. XXXX, XXX, XXX−XXX

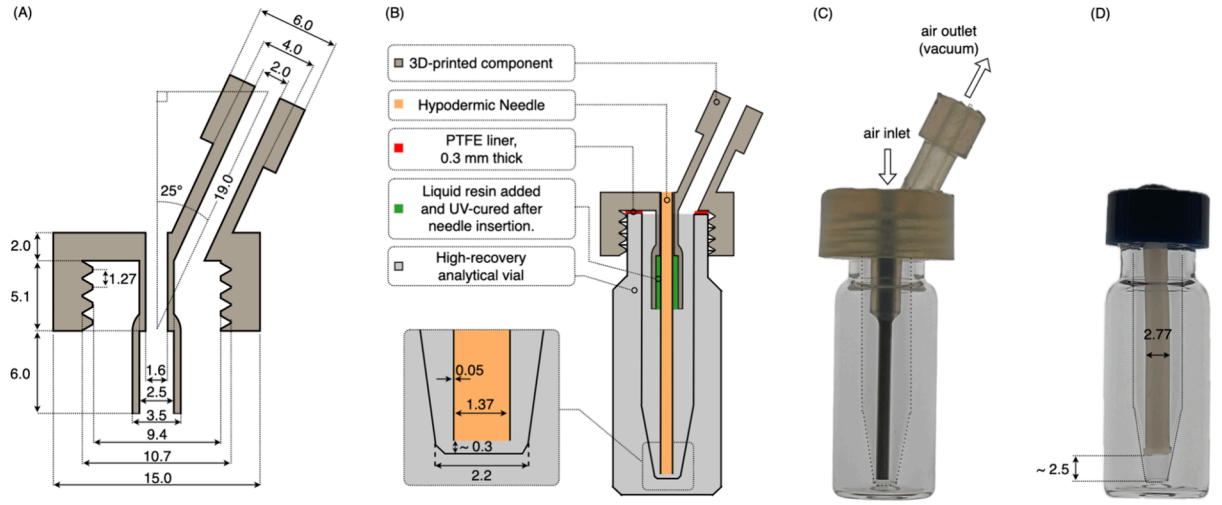

Figure 2. (A) Cross-sectional view and dimensions of the 3D-printed impactor part; (B) Diagram of the impactor assembly; (C) Photograph of the assembled impactor; and (D) Photograph of the microreactor assembly. All dimension units are in millimeters (mm). See Experimental Section for details.

ID# IRB001967), and the volunteers provided written consent to participate in the study. In contrast to sampling of exhaled breath condensate, where gaseous emissions from the stomach and esophagus can be extensive, exhaled breath particles do not yield such contamination. Therefore, no dietary restrictions or fasting protocols were implemented.

Prior to each sample collection, the chamber was filled with 80 L of anhydrous ultraclean air, resulting in a RH of ~1%. Then, the volunteer, after spending a minimum of 1 min in the clean air enclosure to remove ambient atmospheric particles from the lung, entered breath from *ca.* 25 deep exhalation maneuvers into the bag, until the RH reached ~60% at a temperature of 23 °C. Assuming RH of deep-exhaled breath to be ~99% at 35 °C, this corresponds to about 40 L of exhaled air. The contents of the bag were then allowed to sediment for a duration of 1 min, which served to remove any larger particles that might have been generated in the oral cavity. Following this step, aerosol size and concentration inside the chamber were monitored using the TSI-3330 optical particle sizer, operating at a low flow rate of 1 L/min. Aerosols were collected either on a 3-μm PTFE syringe filter (TISCH Scientific, SF18276) or using a custom impactor described below. While flow rates as high as 7.9 L/min were achieved for filter collections, the impactor operated optimally at a flow rate of 4.7 L/min. At these flow rates, samples were collected for 13 and 20 min for the filter and impactor, respectively. Samples collected on PTFE filters were processed immediately after collection. Dehydrated particles collected by impaction at the bottom of mass spectrometry vials were stored at 4 °C for up to 3 days before derivatization.

Preparation of Sodium-Free 70% Ethanol. A mixture of D_2O (12 mL, Sigma-Aldrich, DLM-4−99−1000), ethanol (28 mL, Sigma-Aldrich, 1.00983.1011), and mixed bed ion-exchange resin (0.8 g, Sigma-Aldrich, 13686-U) was shaken overnight at 220 rpm and 37 °C in a 50 mL polyethylene Falcon tube. Immediately after this step, the solution was tested by ^{23}Na NMR to confirm the absence of detectable sodium. The prepared solution was stored at room temperature in the polyethylene container and contact with any glass surfaces was strictly avoided. Polyethylene pipet tips were used for sample handling to exclude sodium contamination.

Sample Preparation for ^{1}H and ^{23}Na Measurements. Samples for sodium and phosphatidylcholine (PC) measurements were collected on PTFE syringe filters. Prior to each sampling, the filters were washed using 2 mL of sodium-free 70% ethanol. They were then mounted on a syringe tip connected to a sampling vacuum line and inserted in the chamber through its sampling port (Figure 1C). Samples were collected on the filters by drawing air from the bag through the filter in the reverse direction. Once the sampling was finished, the filter was removed and flushed slowly in the normal direction with 0.5 mL sodium-free 70% ethanol, dispensed directly into fused-silica 5 mm NMR tubes (Norell NORS55-00QTZ7). The actual volume of the wash solvent was determined gravimetrically by weighing the NMR tube before and after the wash. First, ^{23}Na NMR measurements were carried out using a Bruker Avance-2 600-MHz NMR spectrometer, equipped with a room-temperature broad-band inverse probehead, using 3,145,728 scans (~17 h). Then, 1 μL ammonia solution (30% v/v, Sigma, #105423) was added to the NMR sample, and ^{1}H NMR spectra were obtained. The ammonia addition served to accelerate the base-catalyzed hydrogen exchange of water and ethanol hydroxyl protons, resulting in a sharp, well-defined lock signal. The pulse sequence used a nonselective 90° excitation pulse, followed by a frequency-selective refocusing pulse on the choline methyl resonance, surrounded by a pair of pulsed field gradients (see SI for pulse program). A total of 128 transients were acquired, with a repetition rate of 30 transients per minute (~4.5 min). The ^{1}H NMR resonance intensity of the trimethyl singlet of the PC moiety (3.26 ppm; referenced to sodium trimethylsilylpropanesulfonate) was used for quantification. The ^{1}H NMR spectra were recorded on a Bruker Neo 600-MHz spectrometer, equipped with a pulsed-field-gradient cryogenic probehead.

Impactor Construction. The impactor consists of (1) a high-recovery analytical vial (Agilent, 5188-6591), (2) a stainless steel needle, made of hypodermic tubing, directing the sampled air to the bottom of the vial, (3) a 3D-printed resin part with threading that matches both the vial to hold the needle in place and an outlet for vacuum connection, and (4) a PTFE liner that seals the assembly (Figure 2). The impactor

https://doi.org/10.1021/acs.analchem.4c06422
Anal. Chem. XXXX, XXX, XXX−XXX

was printed via stereolithography on a 3D printer (Formlabs, Form 3+) using standard resin (Formlabs, Durable). The printed part was thoroughly washed with isopropanol before assembly. A ∼ 35 mm segment of hypodermic tubing (ID: 1.37 mm, OD: 1.47 mm, MicroGroup, 304H17XX), was inserted and liquid resin was added around this needle in the bottom cup (colored green in Figure 2B) to provide support and create an airtight seal. The assembly was then cured upside down for 1 h at 60 °C using a curing chamber (Formlabs, Form Cure). After securing the hypodermic tubing segment, a 250-μm thickness PTFE liner (colored red in Figure 2B) was inserted into the cap; this noncompressible liner helps maintain a consistent clearance of about 300 μm between the tubing and the vial bottom. The tubing length was fine-tuned with sandpaper to ensure precise alignment.

Urea Derivatization Reagent. The reagent solution was prepared at ambient temperature immediately before each derivatization reaction by mixing the following components: (1) 40 μL of a ninhydrin stock solution (50 mM), (2) 8 μL of ^{15}N-labeled urea solution in water (0.5 mM), (3) 152 μL of water, and (4) 200 μL of HPLC-grade acetonitrile (Fisher Chemical, A998SK-4). This yielded a 400 μL reaction mixture with final concentrations of 5 mM ninhydrin and 10 μM ^{15}N-urea in a 1:1 acetonitrile:water solvent system.

The above 50-mM ninhydrin stock solution was prepared freshly before each experiment due to its instability, by dissolving solid ninhydrin (4.45 mg, Sigma-Aldrich, 102679996) in aqueous sodium carbonate solution (0.5 mL, 100 mM). The pH of this solution was measured to be ∼9.9 using a glass electrode. Ninhydrin dissolves slowly in water and was mixed by vortexing without heating or sonication to avoid side reactions that can occur under basic or heated conditions. The 0.5 mM ^{15}N-urea solution was stored at −20 °C and thawed prior to each experiment for immediate use. Milli-Q water (18 MΩ·cm) was used as the water source throughout this study.

Urea Derivatization in Microreactor. After sample collection using the impactor, 3 μL of the urea derivatization reagent described above was added to the bottom of each vial using a 10-μL glass syringe (Sigma-Aldrich, 20779). A PTFE rod (diameter: 2.77 mm, length: 29 mm, McMaster-Carr, 84935K86) was then inserted into the conically shaped bottom of the vial. The vial cap (Agilent, 5182−0717) was secured tightly to press against the PTFE rod, creating an airtight seal near the bottom of the vial to prevent solvent evaporation from the total reactor volume of *ca* 10 μL. The vials were then heated at 50 °C for 5 h using a heating block (Fisher Scientific ISOTERM-125D). A custom-made aluminum block with round slots (diameter: 12.0 mm, depth: 23.5 mm) was used to accommodate the high-recovery vials.

After heating, the vials were cooled to room temperature, and 60 μL of 0.2% formic acid (Sigma-Aldrich, 33015) in Milli-Q water was added to each vial. The tip of the PTFE plunger was immersed a few times into the solution to minimize adhered reaction components. The diluted samples were then stored at −20 °C and were thawed without heating and thoroughly mixed prior to LC-MS analysis.

LC-MS Analysis. Quantification of derivatized urea was achieved by ultraperformance liquid chromatography-tandem mass spectrometry (UPLC-MS/MS) utilizing a Thermo Scientific Vanquish UPLC with a Thermo Scientific Altis triple quadrupole mass spectrometer and heated electrospray ionization (HESI-II) in positive ion mode (3850 V). Separation was conducted using a low-coverage C18 stationary phase (Waters UPLC HSS T3 1.8 μm, 2.1 × 100 mm,186003539) maintained at 30 °C, with a mobile phase consisting of solvent A: water and solvent B: acetonitrile, both containing 0.1% formic acid.

A 5 μL aliquot was injected at 5% B and a flow-rate of 200 μL/min, followed by gradient steps: hold 5% B for 0.25 min, 5 to 95% B from 0.25 to 5.5 min, hold 95% B up to 7.5 min, 95 to 5% B from 7.5 to 8 min and hold 5% B up to 10 min. Heated electrospray ionization was conducted with a Sheath gas of 40, Aux gas 7, Sweep gas 2, Ion transfer tube temperature 325 °C and vaporization temperature of 275 °C.

Detection and quantitation of natural ^{14}N-derivatized urea and internal standard ^{15}N-derivatized urea were based on multiple reaction monitoring (MRM) quantitation and confirming transitions m/z 221.1 → 160.1 and 133.0 and 223.1 → 161.1 and 133.0, respectively. Quantitation was performed with Chromeleon (version 7.2.10, Thermo Scientific), a calibration range from 1 nM to 1000 nM with a minimum $R^2 \geq 0.99$ with 1/x weighting, meeting FDA LC-MS guidelines for linearity and quantitation.

RESULTS AND DISCUSSION

For our measurements, we collected exhaled breath into a flexible-sized chamber that was partially prefilled with anhydrous ultraclean air. The mixing of breathing air, saturated with water vapor at body temperature, with the dry air resulted in rapid dehydration of breath droplets.[28] The subject exhaled into the bag until the RH in the chamber reached 60%, well below the DRH of breath aerosols. Maintaining RH below the DRH ensures reproducible particle characterization using an optical particle sizer, as particle size shows only a minimal dependence on RH below this threshold. Another advantage of keeping the particles dry is that their lower size increases their airborne lifetime, allowing sufficient time for characterization and collection. In a still-air environment, particles fall at a terminal Stokes velocity, v, that is determined by their size: $v \approx 0.1\ D^2$ m/h, where D is the particle diameter in μm. For instance, a 1-μm particle can remain airborne for many hours, whereas a 10-μm particle descends 1 m in just 6 min.

The buffering nature of a flexible chamber, as opposed to a rigid container, enables addition of the exhaled breath to the ultraclean, dry air, at arbitrary exhalation rates, independent from the flow rates of the particle sizer and aerosol collection devices. However, a flexible chamber with walls consisting of organic polymer that easily accumulates static charge resulted in rapid electrostatic aerosol deposition. Instead, we used a static-shielding material typically used for packaging electronic devices. It consists of an aluminized polyester layer wrapped in polyethylene material with additives that prevent static build up. By adapting this material, we minimized total particle volume loss during sampling, even for sampling durations up to 20 min at which point the chamber had collapsed nearly completely (Figure 3).

The particle size distribution generated by the deep exhalation maneuvers (Figure 4) concurs with results from previous studies.[13,29,23] Although the vast majority of particles have submicron diameters, particles with $D \geq 1$ μm dominate the total particle volume since volume scales with the cube of the particle diameter. This observation is particularly relevant for cases where filters are incompatible with the analyte of interest. In such situations, impactors, which are more efficient

https://doi.org/10.1021/acs.analchem.4c06422
Anal. Chem. XXXX, XXX, XXX−XXX

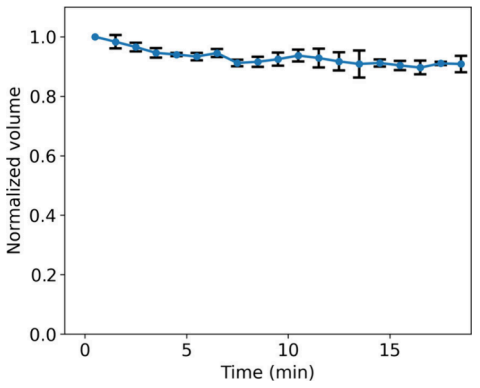

Figure 3. Stability of exhaled breath particles in the chamber during typical sample collection. Total particle volumes are normalized to the first time point. Error bars represent standard deviations over three measurements.

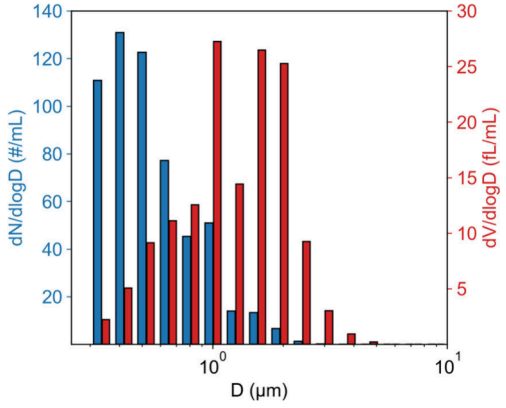

Figure 4. Example of breath particle distribution in the chamber as a function of their diameter, D. Particle counts (blue) and volumes (red) are reported per mL of exhaled air, normalized in the standard manner by the derivative of their diameter logarithm. The mean of optical particle sizer bin boundaries was used for volume calculations; refer to the supporting material for bin cutoff points.

at collecting larger, micron-sized particles offer a more suitable alternative (*vide infra*).

Aerosol Collection Using a PTFE Filter. Once aerosols are introduced into the chamber, they can be collected using a variety of air sampling techniques. A wide range of bioaerosol sampling methods has been employed in the literature, each with distinct advantages and limitations.[30] These methods typically rely on principles such as impaction, centrifugal force, condensation, and filtration, or a combination thereof. Among these, filters made of appropriate materials and pore sizes are particularly efficient, especially when maintaining microbial viability is not a primary concern. For instance, a 3-μm PTFE filter has been demonstrated to collect particles over a wide range of sizes with near-quantitative efficiency.[31] In our study, we utilized such a filter as one of two methods to capture breath aerosols. After collection, the filters were washed with a 0.5 mL 70:30 ethanol:D_2O (v/v) solvent mixture. This composition was selected for two reasons: (1) it effectively wetted the filter, ensuring thorough elution of the collected material, and (2) it efficiently solubilized hydrophobic lipids present in the airway lining fluid. The near complete elution of the samples was verified by obtaining both ^{1}H and ^{23}Na NMR spectra of the second wash of the largest breath samples collected in this study (see SI Figures S1 and S2).

Sodium Measurement. Quantitative assessment of the concentration of analytes in ELF from dehydrated breath particles requires measurement of a reference analyte whose concentration in ELF is firmly established. Considering its tightly controlled value of 122 $\pm$ 2 mM,[26] the use of ^{23}Na for this purpose is a logical choice.[32] We exploit the quantitative nature of NMR for measuring analytes in cases where sensitivity is not a limiting factor. ^{23}Na has spin 3/2, and 100% natural abundance. However, its small gyromagnetic ratio results in relatively low NMR sensitivity. To optimize signal-to-noise gain per unit time, the longitudinal relaxation time of ^{23}Na was measured in our solvent system (11.1 ms; Figure S3), and the repetition time was adjusted accordingly at 50 scans per second. This rapid repetition allowed spectra of sufficient signal-to-noise to be obtained in ~17 h of data collection per sample. Notably, this was achieved using a nonoptimized 30-year-old, broad-band-inverse room temperature probehead.

Environmental prevalence of sodium poses severe contamination challenges when quantifying the nanogram quantities sampled from breath particles. Indeed, in our preliminary experiments, quantification of the low levels of sodium from breath was completely overwhelmed by sodium from solvents and glassware. Therefore, after pinpointing the sources of contamination using ^{23}Na NMR spectroscopy, residual sodium in solvents was removed using ion-exchange resin, and fused silica NMR tubes (also known as quartz tubes) were used to prevent sodium leaching from regular borosilicate NMR tubes into the solution.

Overcoming the background contamination, Figure 5 illustrates the sodium content of breath particles, in nmol,

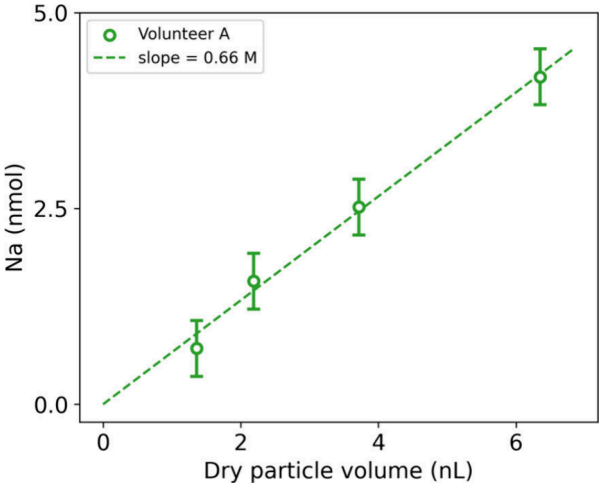

Figure 5. Sodium in breath particles for volunteer A, measured by ^{23}Na NMR, plotted against total dry volume of collected particles, measured by an optical particle sizer. For ^{23}Na NMR spectra, and a corresponding plot of PC methyl intensity, see Figures S1 and S4.

plotted against collected dry particle volume, in nL. The sample size was stepped by collecting particles from increasing numbers of exhaled breaths, totaling 120 to 440 L, on each PTFE filter. In this representation, the slope of the resulting line is the molarity of sodium in dry particle volume, as quantified by the optical particle sizer. Notably, the correlation is linear, with an intercept of zero. This result confirms the absence of background contamination and indicates the sodium concentration in dried aerosols to be 0.66 M. For a

https://doi.org/10.1021/acs.analchem.4c06422
Anal. Chem. XXXX, XXX, XXX−XXX

concentration of 0.12 M ^{23}Na in lung fluid,[26] the hydrated volume of the breath droplets at the time of formation is then estimated to be ~5.5 times larger than the dehydrated particles. This factor is smaller than the 8-fold difference suggested by Nicas et al.,[33] and much smaller than values of ca. 4.5^3 (~90 = fold) reported by Bagheri et al.[18] for droplets produced by singing. As discussed below, the small shrinkage factor observed by us for breath particles likely reflects their enrichment in phospholipids relative to the ELF, possibly related to the mechanism of "bursting films" by which they are generated.

Phospholipid Measurement. Lung fluid contains pulmonary surfactant to prevent collapse of the narrow diameter terminal airways by surface tension when their diameter shrinks during exhalation.[34,35] This surfactant is composed of 90% lipids and about 10% surfactant proteins.[36] Among these lipids, phosphatidylcholines (PCs) such as DPPC are the major components.[34,37] The choline moiety of PCs contains nine equivalent protons, which yield a singlet resonance in their ^{1}H NMR spectrum, enhancing the sensitivity of NMR for their quantification. As was observed for ^{23}Na, the total PC contents measured by NMR correlates linearly with the total collected volume of particles, with an intercept of zero (Figure 6), validating the absence of detectable background contamination.

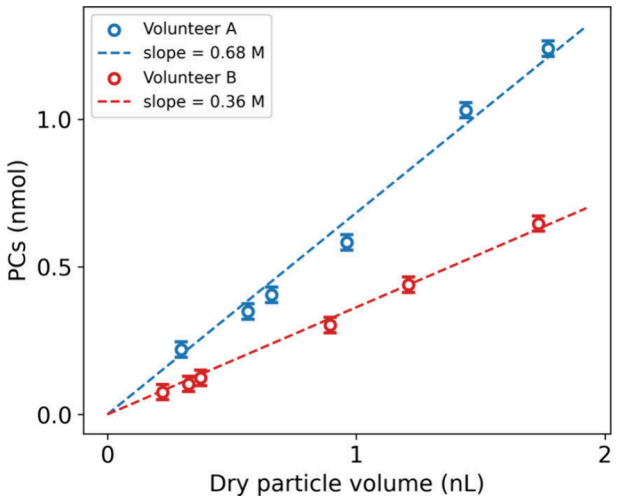

Figure 6. Total phosphocholines (PCs) for volunteers A and B, measured by ^{1}H NMR, plotted against total volume of collected particles, quantified by optical particle sizer.

Measurement of PCs was repeated for two volunteers, A and B, using much smaller total amounts of collected breath. In this case, the sample size was stepped by collecting increasing numbers of breaths on each PTFE filter from 40 to 240 L of exhaled breath. While for both volunteers, the total collected PC quantity scaled linearly with particle volume, the slopes of the two sets of measurements differed substantially (Figure 6). Using the molecular weight of DPPC, the dominant PC species in lung fluid, and assuming a density of 1 g/mL for dry particles, the corresponding weight percentages of PCs for Volunteers A and B were calculated to be 50% and 26%, respectively. The phospholipid fraction observed for volunteer A is in fair agreement with measurements by Hussain-Alkhateeb et al.[37] In their study of 200 subjects, they reported that the combined weight of DPPC, POPC, PC14:0/16:0, and PC16:0/18:2 averaged 46% by weight.[37] On the other hand, the lower value observed for volunteer B is in good agreement with a DPPC wt % of *ca.* 10%, reported by Bake et al.[1] considering that DPPC makes up approximately half of the total PCs in epithelial lining fluid.[7] Importantly, both their and our study observe a PC fraction that appears far higher than the value of ~0.25 wt % in ELF observed by bronchoalveolar lavage (BAL)[38] after accounting for the *ca.* 100-fold dilution[39] of the ELF by the saline rinse. For comparison, PC concentrations measured by us for dehydrated ELF must be scaled down by 5.5-fold, or by 8-fold based on Nicas' analysis,[33] to obtain the concentration in the fluid from which the breath particles were derived. However, they remain more than an order of magnitude higher than the 0.25% w/v observed by BAL. We therefore conclude that the exhaled breath particles are enriched in phospholipids relative to the fluid from which they derive, presumably by the mechanism of 'popping soap films" that underlies their creation.

A comparison of the measured sodium and PC levels for Volunteer A reveals that they are carried in breath droplets in an equimolar ratio (Figures 5, 6, and S4). Whether this observation offers insight into the mechanism of breath particle formation or is only coincidental remains an open question. The reported binding constant of sodium to DPPC liposomes is 0.25 M^{-1} and is comparable to that of other PCs,[40,41] indicating very weak binding between sodium and the DPPC monolayer surface. This suggests that in ELF with a sodium concentration of 0.12 M, only about 3% of DPPC molecules are bound to sodium. Therefore, the observed equimolar ratio is unlikely to result from sodium-PC binding.

Collection of Aerosols by Impaction in a Mass Spectrometry Vial. A major challenge to quantifying metabolites that are present in breath aerosols at very low levels results from background contamination in solvents and reagents, which are needed to derivatize such metabolites for quantitative mass spectrometry. Although filters are highly efficient at collecting aerosols across all sizes, a relatively large amount of solvent (about 0.5 mL in our case) is required to elute the analytes from the filter. In our preliminary attempts to quantify urea, this resulted in noisy correlations between measured urea levels and collected particle volumes, with offsets significantly larger than the expected urea content in breath particles. To address this problem, we developed a sampler based on impaction that collects dry aerosols directly at the bottom of a total recovery mass spectrometry vial with 72 ± 9% efficiency (Figure 2A-C). The conical shape of the vial allows for the insertion of a plunger to run the urea derivatization reaction in a very small volume (3 μL), effectively functioning as a microreactor vessel (Figure 2D). This approach minimizes sample handling and reduces required reagent volumes by more than 2 orders of magnitude, thereby strongly reducing background contamination.

Urea Measurement. Ammonia, a primary waste product of protein breakdown, is converted to urea in the liver to reduce its toxicity. Urea is then removed from the bloodstream by the kidneys. This pathway represents the main mechanism of excess nitrogen removal from the body. Therefore, urea is routinely measured in biological fluids for assessing kidney and liver functions. Plasma samples typically exhibit urea concentrations in the 2−8 mM range with a weak dependence on age,[42] and do not require sensitive methods for quantification. ELF urea levels are in a fairly rapid dynamic equilibrium with plasma levels, and urea measurements of BAL

https://doi.org/10.1021/acs.analchem.4c06422
Anal. Chem. XXXX, XXX, XXX−XXX

fluid therefore are commonly used for quantifying the amount of ELF present in BAL.[39] However, the total volume of ELF collected from breath particles is about 6 orders of magnitude lower, challenging common urea detection methods.

Currently, the most sensitive methods for urea quantification are based on Schiff base complex formation with aldehydes, resulting in UV−vis active complexes.[43] These methods, however, do not reach the sensitivity required for low-biomass breath aerosol samples. Liquid chromatography mass spectrometry (LC-MS) is the method of choice for sensitive quantification of metabolites. However, for small hydrophilic molecules such as urea, derivatization is required to achieve good separation on reversed-phase chromatography followed by unambiguous quantification using MRM mass spectrometry methods. The Schiff-base derivatives discussed above, however, are formed reversibly and decompose to their original components upon dilution required in chromatography methods. Instead, we resorted to the well-documented reaction of urea with ninhydrin,[44,45] forming a stable, two-point adduct between the two. This reaction, along with the use of similar vicinal dicarbonyl compounds, has been investigated for its potential in developing low-cost portable dialysis devices.[44,46] NMR experiments showed that the reaction accelerates at higher pH, but we found that high pH also results in the formation of a side product. This side product exhibits a distinct singlet at 5.36 ppm in the ^{1}H NMR spectrum (referenced to DSS at 50 °C in 10 mM aqueous Na_2CO_3 with 2% D_2O, at pH ∼ 10), suggesting a ring-opening mechanism. At pH ∼ 10 and 50 °C, the urea-ninhydrin reaction accelerates and dominates over the formation of the side product. Therefore, we selected these conditions for the derivatization reaction.

The use of ninhydrin for derivatization in the microreactor vessel drastically reduced background contamination and yielded an approximately linear correlation between the volume of breath particles and the observed urea quantity (Figure 7). Note that the *y*-axis scale is in pmol whereas for sodium and for PCs this was in nmol. The slope of the line is *ca.* 9.3 mM, which corresponds to the urea concentration in the collected dry particles. Using the shrinkage factor of 5.5, this value can be converted to a urea concentration in ELF of 9.3/5.5 = 1.7 mM, which falls at the lower end of the reported range for urea concentrations in plasma.[47] The latter depends on the dietary intake and hydration state of the volunteer, which together with the fact that samples were collected over several weeks explains the wider spread of urea data compared to those of PCs and sodium.

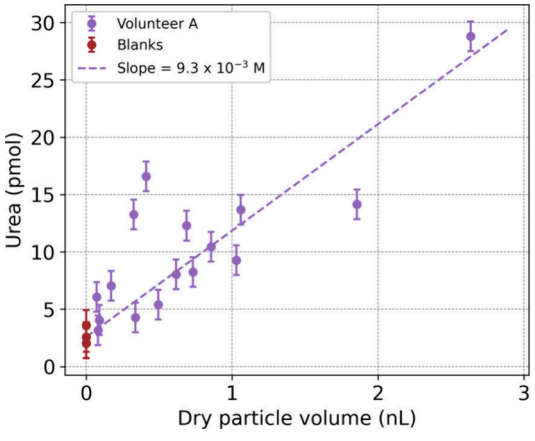

Figure 7. Urea in exhaled breath particles for volunteer A, measured by LC-MS, plotted against total volume of collected particles, measured by optical particles sizer. Samples were collected using impaction in a total recovery mass spectrometry vial, followed by ninhydrin derivatization. Dry particle volumes were corrected for 72% collection efficiency.

NMR Analysis of Phospholipids. While breath particles collected with the PTFE filter enabled measurement of the choline methyl signal for quantitation of phospholipids, impurities in commercially available solvents far exceeded intensities of the other phospholipid NMR signals. However, collection of the aerosols at the bottom of the high-recovery analytical vial by impaction allowed the amount of solvent to be strongly reduced. Indeed, all the previously assigned DPPC glycerol and choline headgroup signals were readily observed without major contaminant interference when dissolved in 30 μL of MeOD (Figure 8). The observed resonances align well with the PC moieties of DPPC and POPC (Figure S5) and are consistent with reference spectra.[48]

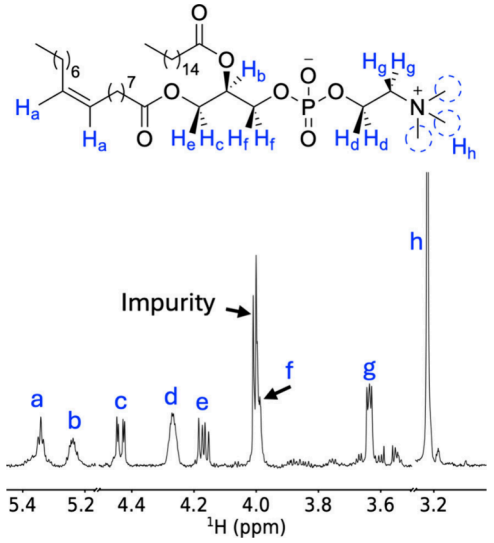

Figure 8. Partial ^{1}H NMR spectrum of exhaled breath particles in methanol-d_4 (MeOD) at 20 °C, referenced to tetramethylsilane. Solvent regions are clipped off for visual clarity. Sample was collected using impaction from 240 L of breath from Volunteer A and suspended in 30 μL of methanol-d_4 with ≥99.96% deuteration. See Figure S5 for the full spectrum and overlays with reference compounds and blank solvent sample.

Comparison of the intensity of glycerol backbone protons with those of the olefinic resonances at 5.34 ppm indicates that roughly 40% of the alkyl chains are unsaturated, in fair agreement with prior analysis of mammalian lung surfactant composition.[49]

CONCLUDING REMARKS

While exhaled breath condensate is very suitable for capturing volatile components, exhaled breath particles in dry form do not retain such molecules. Thus, EBC and EBP sampling protocols are complementary depending on the biomarkers of interest. Although standard EBC sampling devices are inefficient for collecting EBPs,[14] our system has the potential to collect both EBPs and volatile components by placing a

https://doi.org/10.1021/acs.analchem.4c06422
Anal. Chem. XXXX, XXX, XXX−XXX

condenser behind the aerosol samplers, enabling simultaneous analysis of both fractions.

By separating breath collection and aerosol sampling steps, the system described here is compatible with diverse aerosol sampling methods. This sequential approach also accommodates various breathing routines, including deep exhalation maneuver, tidal breathing, high-speed forced exhalation, and even coughing. Furthermore, the chamber's flexibility allows for breath collection under tightly controlled humidity conditions, enabling condensation-based sample collection under their optimal and reproducible conditions, extending functionality beyond the physical collection devices used in this study.

Sodium measurements presented here, for the first time, enable back-calculation of the aqueous volume fraction of breath droplets during their formation. This insight is crucial for downstream biomarker quantification in terms of concentrations in aerosolized lung fluid. The protocol described here overcomes the main challenge in sodium quantification of low-biomass samples, which is background contamination from solvents and glassware. While our sodium measurements required a large volume of exhaled breath, NMR hardware exists that is more sensitive than our old nonoptimized probe by several orders of magnitude.[50] This type of analysis on a larger population in a clinical setting therefore may answer one of the key open questions regarding the physical properties of respiratory particles.[6]

Our strategy of collecting aerosols directly into a microreactor for subsequent derivatization addresses a key challenge in analysis of low-biomass samples: background contamination. This method is particularly pertinent for cases where solvent or handling-related contamination is a serious concern, since the collected dry sample can be directly suspended in a minimal amount of any desired solvent or derivatization reagent. Its successful application in quantifying urea in exhaled breath particles highlights the practical advantages of this method. This advance is pivotal for quantification of a wide range of biomarkers, including short chain fatty acids that are of high biological interest, but currently cannot be reliably quantified from lung fluids due to contamination issues.[25]

Accurate characterization of exhaled breath particles prior to collection for chemical analysis enables quantitative analysis of lung fluid biomarkers. This approach overcomes the issue of unknown dilution that limits reproducibility in other lung sampling methods, such as induced sputum, exhaled breath condensate, and BAL washes. The low-cost, noninvasive system described in this study simplifies further method development studies for metabolite and possibly microbiome analysis in lung fluid. Our approach contrasts with analysis of BAL fluid, which requires a trained physician, anesthesia, and a medical setting.

■ ASSOCIATED CONTENT

Supporting Information

The Supporting Information is available free of charge at https://pubs.acs.org/doi/10.1021/acs.analchem.4c06422.

Additional sodium and phosphocholine-methyl NMR spectra; Na NMR relaxation data; plot of phosphatidylcholine vs dry breath particle volume; comparison of ^{1}H breath particle NMR spectra with solvent blank, POPC and DPPC spectra; 2D DQF-COSY spectrum of breath particles; calibration plot and LC-MS chromatogram of the urea-ninhydrin adduct; NMR pulse sequences; bin cutoff values used for the optical particle sizer (PDF)

The .stl file of the impactor device (ZIP)

■ AUTHOR INFORMATION

Corresponding Authors

Tayeb Kakeshpour − *Laboratory of Chemical Physics, National Institute of Diabetes and Digestive and Kidney Diseases, National Institutes of Health, Bethesda, Maryland 20892, United States*; Email: Tayeb.Kakeshpour@gmail.com

Ad Bax − *Laboratory of Chemical Physics, National Institute of Diabetes and Digestive and Kidney Diseases, National Institutes of Health, Bethesda, Maryland 20892, United States*; orcid.org/0000-0002-9809-5700; Email: bax@NIH.gov

Authors

John M. Louis − *Laboratory of Chemical Physics, National Institute of Diabetes and Digestive and Kidney Diseases, National Institutes of Health, Bethesda, Maryland 20892, United States*; orcid.org/0000-0002-0052-1899

Peter J. Walter − *National Institute of Diabetes and Digestive and Kidney Diseases, Clinical Mass Spectrometry Core, National Institutes of Health, Bethesda, Maryland 20892, United States*

Complete contact information is available at: https://pubs.acs.org/10.1021/acs.analchem.4c06422

Notes

The authors declare no competing financial interest.

■ ACKNOWLEDGMENTS

The authors thank Dr. Philip A. Anfinrud for providing clean room space and Bernard Howard for assistance in the workshop. The authors also thank Drs. Hyomoon Cho, Carole A. Bewley, John R. Lloyd, Juan M. Lopez and Marshall Smith for discussions, Drs. James Baber and Jinfa Ying for NMR technical support, Ms. Nancy Alexander for assistance with the IRB exemption request, and Dr. Dennis Torchia for comments on the manuscript draft. This work was supported by the Intramural Research Program of the National Institute of Diabetes and Digestive and Kidney Diseases.

■ REFERENCES

(1) Bake, B.; Larsson, P.; Ljungkvist, G.; Ljungstrom, E.; Olin, A. C. Exhaled particles and small airways. *Respir. Res.* **2019**, *20*. DOI: 10.1186/s12931-019-0970-9

(2) Johnson, G. R.; Morawska, L. *J. Aerosol Med. Pulm. Drug Delivery* **2009**, *22* (3), 229−237.

(3) Almstrand, A.-C.; Bake, B.; Ljungström, E.; Larsson, P.; Bredberg, A.; Mirgorodskaya, E.; Olin, A.-C. *J. Appl. Physiol.* **2010**, *108* (3), 584−588.

(4) Holmgren, H.; Ljungstrom, E.; Almstrand, A. C.; Bake, B.; Olin, A. C. *J. Aerosol Sci.* **2010**, *41* (5), 439−446.

(5) Scheideler, L.; Manke, H.-G.; Schwulera, U.; Inacker, O.; Hammerle, H. *Am. J. Respir. Crit. Care Med.* **1993**, *148* (3), 778−784.

(6) Morawska, L.; Buonanno, G.; Mikszewski, A.; Stabile, L. *Nature Reviews Physics* **2022**, *4* (11), 723−734.

(7) Larsson, P.; Holz, O.; Koster, G.; Postle, A.; Olin, A.-C.; Hohlfeld, J. M. *BMC Pulm. Med.* **2023**, *23* (1), 423.

(8) Pauling, L.; Robinson, A. B.; Teranishi, R.; Cary, P. *Proc. Natl. Acad. Sci. U. S. A.* **1971**, *68* (10), 2374−2376.

(9) Horvath, I.; Barnes, P. J.; Loukides, S.; Sterk, P. J.; Hogman, M.; Olin, A. C.; Amann, A.; Antus, B.; Baraldi, E.; Bikov, A.; Boots, A. W.; Bos, L. D.; Brinkman, P.; Bucca, C.; Carpagnano, G. E.; Corradi, M.; Cristescu, S.; de Jongste, J. C.; Dinh-Xuan, A. T.; Dompeling, E.; Fens, N.; Fowler, S.; Hohlfeld, J. M.; Holz, O.; Jobsis, Q.; Van De Kant, K. V.; Knobel, H. H.; Kostikas, K.; Lehtimaki, L.; Lundberg, J.; Montuschi, P.; Van Muylem, A.; Pennazza, G.; Reinhold, P.; Ricciardolo, F. L. M.; Rosias, P.; Santonico, M.; van der Schee, M. P.; van Schooten, F. J.; Spanevello, A.; Tonia, T.; Vink, T. J. *Eur. Respir. J.* **2017**, *49* (4), 1600965.
(10) Effros, R. M. *Chest* **2010**, *138* (3), 471−472.
(11) Effros, R. M.; Hoagland, K. W.; Bosbous, M.; Castillo, D.; Foss, B.; Dunning, M.; Gare, M.; Lin, W. E. N.; Sun, F. *Am. J. Respir. Crit. Care* **2002**, *165* (5), 663−669.
(12) Edwards, D. A.; Man, J. C.; Brand, P.; Katstra, J. P.; Sommerer, K.; Stone, H. A.; Nardell, E.; Scheuch, G. *Proc. Natl. Acad. Sci. U. S. A.* **2004**, *101* (50), 17383−17388.
(13) Holmgren, H.; Ljungström, E.; Almstrand, A.-C.; Bake, B.; Olin, A.-C. *J. Aerosol Sci.* **2010**, *41* (5), 439−446.
(14) Wang, L.; Deng, J.; Wang, D.; Chen, M.; Li, X.; Lu, Y.; Jiang, J. *Aerosol and Air Quality Research* **2022**, *22* (6), 220049.
(15) Almstrand, A.-C.; Ljungström, E.; Lausmaa, J.; Bake, B.; Sjövall, P.; Olin, A.-C. *Anal. Chem.* **2009**, *81* (2), 662−668.
(16) Roe, T.; Silveira, S.; Luo, Z.; Osborne, E. L.; Senthil Murugan, G.; Grocott, M. P. W.; Postle, A. D.; Dushianthan, A. *Diagnostics* **2024**, *14* (10), 972.
(17) Holmgren, H.; Bake, B.; Olin, A.-C.; Ljungström, E. *J. Aerosol Med. Pulm. Drug Delivery* **2011**, *24* (5), 253−260.
(18) Bagheri, G.; Schlenczek, O.; Turco, L.; Thiede, B.; Stieger, K.; Kosub, J. M.; Clauberg, S.; Pohlker, M. L.; Pohlker, C.; Molacek, J.; Scheithauer, S.; Bodenschatz, E. *J. Aerosol Sci.* **2023**, *168*, 106102.
(19) Peng, C.; Chen, L.; Tang, M. *Fundamental Research* **2022**, *2* (4), 578−587.
(20) Pöhlker, M. L.; Pöhlker, C.; Krüger, O. O.; Förster, J. D.; Berkemeier, T.; Elbert, W.; Fröhlich-Nowoisky, J.; Pöschl, U.; Bagheri, G.; Bodenschatz, E.; Huffman, J. A.; Scheithauer, S.; Mikhailov, E. Respiratory aerosols and droplets in the transmission of infectious diseases. *Rev. Mod. Phys.* **2023**, *95* (4). DOI: 10.1103/RevModPhys.95.045001
(21) Roth, A.; Frantz, D.; Stiti, M.; Berrocal, E. *J. Aerosol Sci.* **2023**, *174*, 106257.
(22) Roth, A.; Stiti, M.; Frantz, D.; Corber, A.; Berrocal, E. *Nat. Sci.* **2023**, *3*, No. e20230007.
(23) Morawska, L.; Johnson, G. R.; Ristovski, Z. D.; Hargreaves, M.; Mengersen, K.; Corbett, S.; Chao, C. Y. H.; Li, Y.; Katoshevski, D. *J. Aerosol Sci.* **2009**, *40* (3), 256−269.
(24) Shen, Y.; Courtney, J. M.; Anfinrud, P.; Bax, A. *Proc. Natl. Acad. Sci. U. S. A.* **2022**, *119* (26), No. e2203086119.
(25) Yue, M.; Kim, J. H.; Evans, C. R.; Kachman, M.; Erb-Downward, J. R.; D'Souza, J.; Foxman, B.; Adar, S. D.; Curtis, J. L.; Stringer, K. A. *Am. J. Respir. Crit. Care Med.* **2020**, *202* (4), 610−612.
(26) Song, Y. L.; Thiagarajah, J.; Verkman, A. S. *J. Gen. Physiol.* **2003**, *122* (5), 511−519.
(27) Kakeshpour, T.; Fennelly, K. P.; Bax, A. *Respir. Res.* **2024**, *25* (1), 224.
(28) Netz, R. *J. Phys. Chem. B* **2020**, *124*, 7093−7101.
(29) Tinglev, Å. D.; Ullah, S.; Ljungkvist, G.; Viklund, E.; Olin, A.-C.; Beck, O. *Journal of Breath Research* **2016**, *10* (2), 026001.
(30) Zhang, C.; Dai, X.; Gebrezgiabhier, T.; Wang, Y.; Yang, M.; Wang, L.; Wang, W.; Man, Z.; Meng, Y.; Tong, L.; He, M.; Zhou, B.; Zheng, J.; Xiao, H. *Atmosphere* **2024**, *15* (4), 404.
(31) Burton, N. C.; Grinshpun, S. A.; Reponen, T. *Annals of Occupational Hygiene* **2006**, *51* (2), 143−151.
(32) Effros, R. M.; Biller, J.; Foss, B.; Hoagland, K.; Dunning, M. B.; Castillo, D.; Bosbous, M.; Sun, F.; Shaker, R. *Am. J. Respir. Crit. Care Med.* **2003**, *168* (12), 1500−1505.
(33) Nicas, M.; Nazaroff, W. W.; Hubbard, A. *J. Occup. Environ. Hyg.* **2005**, *2* (3), 143−154.
(34) King, R. J.; Clements, J. A. *American Journal of Physiology-Legacy Content* **1972**, *223* (3), 715−726.
(35) Veldhuizen, R.; Nag, K.; Orgeig, S.; Possmayer, F. *Biochimica et Biophysica Acta (BBA) - Molecular Basis of Disease* **1998**, *1408* (2), 90−108.
(36) Veldhuizen, E. J. A.; Haagsman, H. P. *Biochimica et Biophysica Acta (BBA) - Biomembranes* **2000**, *1467* (2), 255−270.
(37) Hussain-Alkhateeb, L.; Bake, B.; Holm, M.; Emilsson, Ö.; Mirgorodskaya, E.; Olin, A.-C. *BMJ. Open Respiratory Research* **2021**, *8* (1), e000804.
(38) Bégin, R.; Lesur, O.; Bouhadiba, T.; Guojian, L.; Larivée, P.; Melloni, B.; Martel, M.; Cantin, A. *Thorax* **1993**, *48* (8), 840.
(39) Rennard, S. I.; Basset, G.; Lecossier, D.; O'Donnell, K. M.; Pinkston, P.; Martin, P. G.; Crystal, R. G. *J. Appl. Physiol.* **1986**, *60* (2), 532−538.
(40) Tatulian, S. A. *Eur. J. Biochem.* **1987**, *170* (1−2), 413−420.
(41) Satoh, K. *Biochimica Et Biophysica Acta-Biomembranes* **1995**, *1239* (2), 239−248.
(42) Musch, W.; Verfaillie, L.; Decaux, G. *Clin. J. Am. Soc. Nephrol.* **2006**, *1* (5), 909−914.
(43) Zawada, R. J. X.; Kwan, P.; Olszewski, K. L.; Llinas, M.; Huang, S.-G. *Biochem. Cell Biol.* **2009**, *87* (3), 541−544.
(44) Jong, J. A. W.; Smakman, R.; Moret, M.-E.; Verhaar, M. C.; Hennink, W. E.; Gerritsen, K. G. F.; Van Nostrum, C. F. *ACS Omega* **2019**, *4* (7), 11928−11937.
(45) Jong, J. A. W.; Moret, M.-E.; Verhaar, M. C.; Hennink, W. E.; Gerritsen, K. G. F.; van Nostrum, C. F. *ChemistrySelect* **2018**, *3* (4), 1224−1229.
(46) Jong, J. A. W.; Guo, Y.; Hazenbrink, D.; Douka, S.; Verdijk, D.; van der Zwan, J.; Houben, K.; Baldus, M.; Scheiner, K. C.; Dalebout, R.; Verhaar, M. C.; Smakman, R.; Hennink, W. E.; Gerritsen, K. G. F.; van Nostrum, C. F. *Macromol. Biosci.* **2020**, *20* (3), 1900396.
(47) Waters, W. E.; Greene, W. J. W.; Keyser, J. W. *Postgrad. Med. J.* **1967**, *43* (505), 695−700.
(48) Nishida, Y.; Yuan, M.; Fukuda, K.; Fujisawa, K.; Dohi, H.; Uzawa, H. *Beilstein J. Org. Chem.* **2017**, *13*, 1999−2009.
(49) Postle, A. D.; Heeley, E. L.; Wilton, D. C. *Comparative Biochemistry and Physiology Part A: Molecular & Integrative Physiology* **2001**, *129* (1), 65−73.
(50) Sivelli, G.; Conley, G. M.; Herrera, C.; Marable, K.; Rodriguez, K. J.; Bollwein, H.; Sudano, M. J.; Brugger, J.; Simpson, A. J.; Boero, G.; Grisi, M. *J. Magn. Reson.* **2022**, *335*, 107142.

https://doi.org/10.1021/acs.analchem.4c06422
Anal. Chem. XXXX, XXX, XXX−XXX